The Effect of Shot Peening on Additively Manufactured 316L Stainless Steel for the Marine Transportation Industry

L. Bonnici[1], J. Buhagiar[1], G. Cassar[1], K. A. Vella[1], J. Chen[2], X.Y. Zhang[2], M.Y. Liu[2], Z.Q. Huang[2], A. Zammit[1]

1 Department of Metallurgy and Materials Engineering, University of Malta, Msida, Malta
2 School of Materials Science and Engineering, Southeast University, Nanjing, Jiangsu Province, China

Abstract
In the marine transportation industry, the harsh environment during voyage leads to severe corrosion failure or mechanical breakdowns. Hence, continuous and preventive maintenance is required. Additive manufacturing (AM) can potentially be used to reduce the downtime associated with replacement of components by printing the required parts directly from the design itself. In this study, shot peening (SP) was applied as a posterior treatment on AMed 316L stainless steel (SS) with the aim to increase the mechanical properties at the surface and the surface characteristics without creating a detriment to the alloy's corrosion resistance. A 44% increase in surface hardness from 231 $\pm$ 38 $HV_{0.2}$ to 334 $\pm$ 61 $HV_{0.2}$ was measured after SP, while the affected depth was of around 200 µm. SP also resulted in R_a values of 10 $\pm$ 1 µm for as-printed samples, which was reduced to 5 $\pm$ 1 µm after SP. Additionally, the SP treatment induced a surface compressive residual stress of 589 MPa. Corrosion results were not favourable for the SP-ed samples. However, the overall results suggest that the use of AM SP parts may indeed be a suitable contender for use in selected maritime components.

Keywords
Additive manufacturing, shot peening, residual stress measurement, corrosion resistance

Introduction

Maritime activities are the pillar of global economy and trade. Primary necessities such as food, petroleum and goods are imported by means of water transportation. Recent studies show that 70% [1] of the global goods are carried by sea.

The marine environment gives rise to corrosion, erosion and detrimental effects. Due to this, parts such as propellers and shafts must be frequently replaced [2]. The issue of high replacement demands in this industry can be solved with AM. Selective laser melting (SLM) is one of the efficient processes of AM. Parts which are manufactured through SLM are used in various industries such as the medical, dental and aerospace industries, lightweight structures and heat exchangers [3].

However, parts produced via AM have notoriously poor surface finish and high porosity, posing deterioration of such critical parts, weakening their performance, particularly resistance to cyclic loading [4]. To address this challenge, SP was applied to AM 316L SS. Studies performed on polished surfaces, such as that of Sugavaneswaran *et al.* [3], show significant improvements in hardness and roughness following SP.

During this study, samples were left unpolished to deduct a preparation step and also make use of the 3D printer's potential, that which it can manufacture parts rapidly to solve emergent issues. This advantage was explored by Bagherifard *et al.* [5] where a 9% increase in hardness and an 18% reduction in roughness were identified after performing SP on 316L SS. However, in the authors best knowledge, studies on corrosion tests on as-printed and printed and shot peened samples are novel and the aim of this study was to analyse the corrosion properties of unpolished samples amongst other material characterisation studies.

Experimental Methods

316L SS samples were printed with an AmPro SP100 3D Printer, China, using a SLM process. A laser power of 200 W, laser speed of 950 mm/s, beam offset of 10 µm, layer thickness of 30 µm and a hatch distance of 80 µm were used. Table 1 shows the used powder's chemical composition.

Table 1: Chemical composition for powder 316L SS*[6]*

Element	Fe	Cr	Ni	Mo	Si	Mn	P	C	S
wt %	68.64	16.59	10.77	2.48	0.76	0.72	0.025	0.0078	0.0037

SP was carried out using a modified Industrial Surface Treatments sand blaster. S230 steel shots were used, at a pressure of 6 bar, shot flow rate of 50 %, nozzle to specimen distance set to 100 mm, peening time of 21 seconds and intensity of 0.21 mmA. The designation of the samples is AP for the as-printed samples and PSP for the printed and shot peened samples.
Electrochemical tests were carried out with a Gamry Interface 1000™ potentiostat / galvanostat / ZRA. A 3-electrode setup was used. A 1 cm^2 surface area from the sample to be tested was exposed to 300 ml of substitute oceanwater. This was prepared according to ASTM D 1141 – 98: *Standard practice for the preparation of substitute ocean water*. The procedure was comprised of an initial OCP measurement for 2 hours. This was followed by cyclic polarisation sweeps at a rate of 0.167 mV/s between the following ranges: −100 mV versus OCP and -500 mV versus reference. The polarisation scan was instructed to reverse when an apex current of 0.5 mA/cm^2 was reached at a scan rate of 0.167 mV/s. The test was stopped after a few steps once the protection potential was reached. Three repeats were done for each set.
Subsequent material characterisation included optical and scanning electron microscopy, microhardness measurements and topographic analysis. X-Ray Diffractometry (XRD) phase analysis was performed using a Rigaku Ultima IV diffractometer. This was set for Glancing Incidence Asymmetric Bragg (GIAB) with an angle of incidence of 3° and Cross Beam Optics (CBO). The source of radiation used was that of CuKα. The same diffractometer was used to carry out the surface residual stress measurements, set in θ / 2θ configuration. Stresses were measured according to the standard BS EN 15305:2008 - Non-destructive testing - Test method for residual stress analysis by X-ray diffraction. A Rigaku Multipurpose attachment IV (MPA-U4) was used for Ψ tilting and stress measurements were carried out using the parallel beam method. The peak was measured for the [3 1 1] fcc at a theoretical nominal of 2θ = 90.68°. The 2θ range was set from 87° to 93°, with seven Ψ tilts from 0° to 60°.

Experimental Results

Figure 1 shows the microstructure along the building direction of the AP 316L SS to be composed of an austenitic matrix, which was verified by XRD (Figure 3). At higher magnifications, shown in Figure 2, columnar and cellular dendritic structures were observed. Such structures are formed following molten metal solidification.

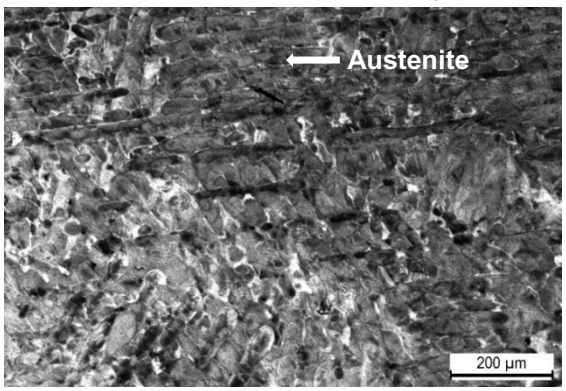

Figure 1: Etched as-printed microstructure highlighting the austenite matrix

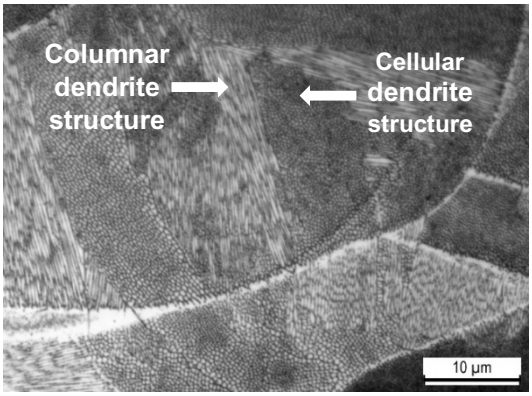

Figure 2: Columnar and cellular dendritic structures in the as-printed microstructure

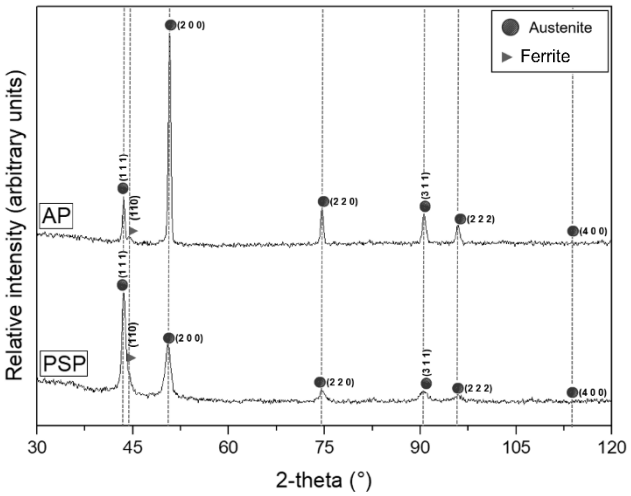

Figure 3: XRD patterns for as-printed and printed and shot peened samples with austenite (PDF number: 00-023-0298) and ferrite (PDF number: 00-003-0411) as the main peaks

Table 1 shows the results obtained in this work. Shot peening resulted in a reduction of 50% for the R_a and 77% for the R_z roughness. This result can also be observed from Figure 4, where the shot peened surface (Figure 4b), showing the individual dimple characteristic, shows to be less rough than the AP surface (Figure 4a) which shows the printing striations. In addition, SP generated a compressive residual stress of 589 MPa at the surface and a 45% increase in surface micro-hardness. The micro-hardness depth profile in Figure 5 shows a maximum hardness value at the surface reaching 334 ± 16 $HV_{0.2}$ decreasing gradually into the bulk, reaching the substrate average hardness of 230 ± 10 $HV_{0.2}$ at around 200 µm.

Table 1: Summary of results for as-printed and printed and shot peened specimens

	n, population for standard error	As-Printed (AP)	Printed and Shot Peened (PSP)
Surface stress (MPa)	2	60 ± 18	-589 ± 9
R_a (µm)	20	10 ± 1	5 ± 1
R_z (µm)	20	95 ± 9	20 ± 5
Surface micro-hardness (HV_{200})	15	231 ± 10	334 ± 16
E_{corr} (mV)	3	-2 ± 14	-198 ± 15
Breakdown potential (mV)	3	500 ± 36	334 ± 92
Protection potential (mV)	3	-133 ± 17	-53 ± 17

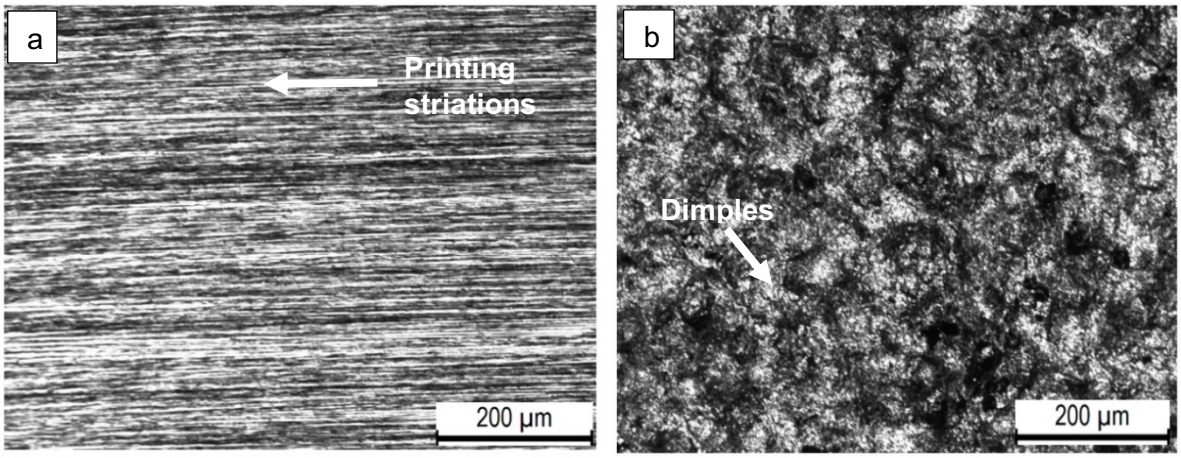

Figure 4: a) As-printed surface, highlighting the printing striations b) Printed and shot peened surface, highlighting the dimples

Figure 6 shows the representative cyclic polarisation curves for AP and PSP, with the marked E_{corr}, breakdown voltage (E_{break}) and protection voltage (E_{prot}). Upon inspecting the respective values in Table 1, it can be seen that AP performed better during the corrosion test than PSP.

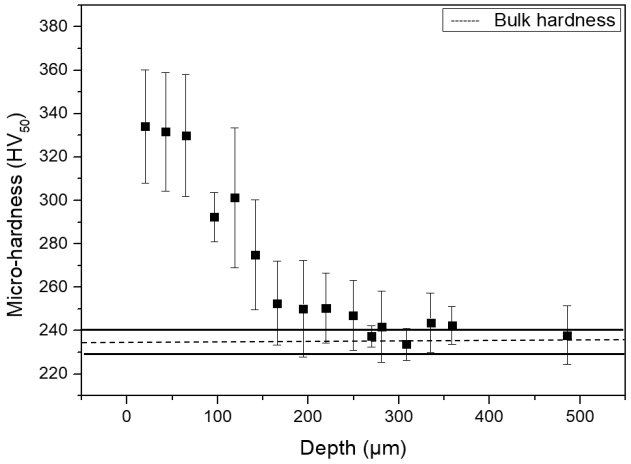

Figure 5: Micro-hardness depth profile for printed and shot-peened

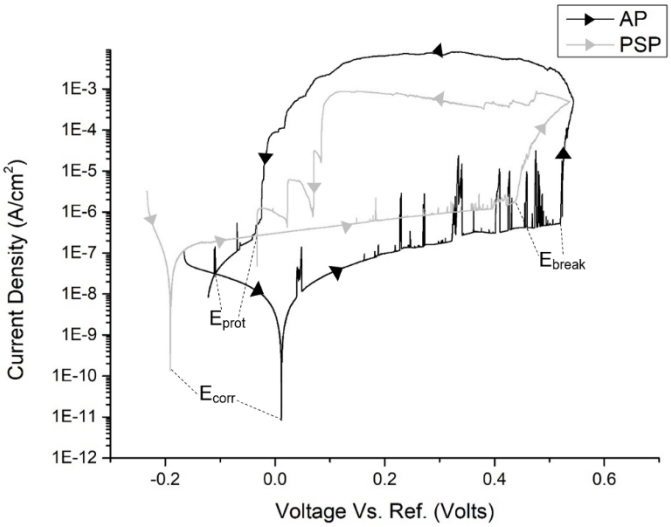

Figure 6: Representative cyclic polarization curves for as-printed and printed and shot peened samples

Discussion and Conclusion

The microstructure of AM 316L SS is made from austenite. Figure 3 shows a peak of ferrite at an angle of 44.5° [1 1 0]. Similar observations were reported for studies performed on 316L SS manufactured by SLM by Sun *et al.* [7], Kurzynowski *et al.* [8] and Kamariah *et al.* [9] . Columnar and cellular dendritic structures were evident, which are attributed to the effect of laser melting during the AM process. These structures were also evident in a study by Jin Oh *et al.* [11] while studying AMed 316L SS.

Following SP, no peak shifts occurred. However, the peak at 44.5° [1 1 0] could be either ferrite or martensite or a mixture of both, as found by Krawczyk *et al.* [12]. This could be a result of the strain induced by the SP. The main differences identified between the AP and PSP diffractographs (Figure 3) were the broadening of XRD peaks in the SP-ed sample and change in relative intensity at the [1 1 1] and [2 0 0] peaks. The broadening of the peaks is attributed to the residual stresses generated. In a study carried out by AlMangour and Yang [13], it was explained that this broadening is formed by plastic deformation leading to macro and micro residual stresses induced by peening. Additionally, the decrease in peak intensity is attributed to the structural change at crystalline level which is caused by severe surface deformation via peening. Prabhakaran *et al.* [14] argue that the reason for such phenomenon is that residual stresses affect the crystal lattice structure and therefore, the lattice spacing. Moreover, the original surface stresses of AP were in the tension state, which were generated during characteristic fast melting and solidification processes. However, SP has resulted in the generation of compressive stresses reflecting the transfer of shot kinetic energy to retained elastic stress, as already explained.

The surface characteristics were also significantly changed after SP. The surface peaks that were present before peening, were flattened, leaving individual and dense dimple characteristics of SP. The features show approximately constant dimensions, confirming the uniformity in the shot sizes and impact velocities. Peak flattening was confirmed by the surface topography results, where a decrease of 50% and 77% were discovered for R_a and R_z respectively. As the shots impinge the surface, the crest is crushed, diminishing the surfaces' roughness. Similar results were obtained in a study performed by Bagherifard *et al.* [5] where unpolished 316L SS was shot peened with S230 shots and an 18% decrease in R_a was found.

Even though there was no full phase transformation, an increase in hardness following SP was still evident. This is due to the cold work taking place as the shots impact the surface. As this is done, plastic deformation takes place, inhibiting any crack formation or propagation, strengthening and hardening the material. These results are comparable to those found by AlMangour *et al.* [13] where a 52% increase in hardness was discovered following SP 17-4 stainless steel. The relationship of the hardness along the depth shows that SP effects a 200 μm depth, which decreases steadily towards the substrate's bulk, proving that there is still subsurface hardening.

When analysing the corrosion results, AP shows more favorable conditions than those for PSP. This was confirmed from the results obtained in Table 1. The higher E_{corr} for AP shows a more corrosion resistant material, while a higher breakdown potential shows a more pitting resistant material. The detrimental effects of PSP could be influenced by the change in surface morphology by creating a larger surface area by the dimples, possibility of multiple phases of ferrite and martensite [15] and also, due to high dislocation densities [16] induced by the SP process [17].

From this study, it can be concluded that SP can be adopted on additively manufactured 316L SS, resulting in an increase in hardness and a decrease in surface roughness. This suggests that SP can be considered as an appropriate surface engineering technique for a number of applications relevant to the marine transportation industry. However, the adverse behavior noted for its corrosion performance should be the subject to further surface engineering treatment, in addition to SP.

Acknowledgments

This study was part of the SEAM project, funded by the Malta Council for Science and Technology (MCST) as part of the Sino-Malta fund 2019-02.

References

[1] J. Hoffmann, "Review of Maritime Transport," in *United Nations Conference on Trade and Development*, New Yord and Genova, 2018.

[2] J. Sienkiewicz and T. J. Cuff, "Extreme Maritime Weather: Improving Safety of Life at Sea," World Meteorological Organization, [Online]. Available: https://public.wmo.int/en/resources/bulletin/Products_and_services/Extereme_maritime_weather. [Accessed 22 May 2022].

[3] M. Sugavaneswaran, A. Vinoth Jebaraj, B. Kumar, K. Lokesh and A. J. Rajan, "Enhancement of surface characteristics of direct metal laser sintered stainless steel 316L by shot peening," *Surfaces and Interfaces,* vol. 12, pp. 31-40, 2018.

[4] H. Bikas, P. Stavropoulos and G. Cryssaolouris, "Additive manufacturing methods and modelling approches: a criticl review," *International Journal of Additive Manufacturing Technology,* vol. 83, pp. 389-405, 2016.

[5] S. Bagherifard, S. Slawik, I. Fernandez-Pariente, C. Pauly, F. Muclich and M. Guagliano, "Nanoscale surface modification of AISI 316L stainless steel by severe shot peening," *Materials and Design,* vol. 102, pp. 68-77, 2016.

[6] J. V. A. M. T. C. Ltd., *Certificate of Quality 316L Stainless Steel,* Suqian, Jiangsu: Jiangsu Vilory Advanced Materials Technology Co. Ltd., 2021.

[7] Z. Sun, X. Tan, S. B. Tor and W. Y. Yeong, "Selective laser melting of stainless steel 316L with low porosity and high build rates," *Materials and Design,* vol. 104, pp. 197-204, 2016.

[8] T. Kurzynowski, K. Gruber, W. Stopyra, B. Kuznicka and E. Chlebus, "Correlation between process parameters, microstructure and properties of 316 L stainless steel processed by selective laser melting," *Materials Science and Engineering A,* vol. 718, pp. 64-73, 2018.

[9] M. Kamariah, W. Harun, N. Khalil, F. Ahmad, M. Ismail and S. Sharif, "Effect of heat treatment on mechanical properties and microstructure of selective laser melting 316L stainless steel," in *4th International Conference on Mechanical Engineering Research* , Malang, Indonesia, 2017.

[10] L. E. Murr, E. Martinez, J. Hernandez, S. Collins, K. N. Amato, S. M. Gaytan and P. W. Shindo, "Microstructures and Properties of 17-4 PH Stainless Steel Fabricated by Selective Laser Melting," *Journal of Materials Research and Technology,* vol. 1, no. 3, pp. 167 - 177, 2012.

[11] W. Jin Oh, W. Jin Lee, M. Seon Kim and J. S. S. D. Bae Jeon, "Repairing additive-manufactured 316L stainless steel using direct energy deposition," *Optics and Laser Technology,* vol. 117, pp. 6-17, 2019.

[12] B. Krawczyk, P. Cook, J. Hobbs and D. L. Engelberg, "Corrosion behaviour of cold-rolled type 316L stainless steel in HCl containg environments," in *Corrosion*, Houston, 2017.

[13] B. AlMangour and J.-M. Yang, "Improving the surface quality and mechanical properties by shot-peening of 17-4 stainless steel fabricated by additive manufacturing," *Materials and Design,* vol. 110, pp. 914-924, 2016.

[14] S. Prabhakaran, A. Kulkarni, G. Vasanth, S. Kalainathan, P. Shukla and V. Vasudevan, "Laser shock peening without coating induced residual stress distribution, wettability characteristics and enhanced pitting corrosion resistance of austenitic stainless steel," *Applied Surface Science,* vol. 428, pp. 17-30, 2018.

[15] L. Peguet, B. Malki and B. Baroux, "Effect of austenite stability on the pitting corrosion resistance of cold worked stainless steel," *Corrosion Science,* vol. 51, pp. 493-498, 2009.

[16] M. Godec, C. Donik, A. Kocijan, B. Podgornik and D. Skobir Balantic, "Effect of post-treated low-temperature plasma nitriding on the wear and corrosion resistance of 316L stainless steel manufactured by laser powder bed fusion," *Additive Manufacturing,* vol. 32, 2020.

[17] S. Geng, J. Sun and L. Guo, "Effect of sandblasting and subsequent acid pickling and passivation on the microstructure and corrosion behavior of 316L stainless steel," *Materials and Design,* vol. 88, pp. 1-7, 2015.